

Gamma decay of $g_{9/2}$ isobaric analog resonance in ^{57}Co

C. Rangacharyulu, I. M. Szöghy, C. St-Pierre, and K. Ramavataram*

Département de Physique et Laboratoire de Physique Nucléaire, Université Laval, Québec G1K 7P4, Canada

(Received 6 March 1978; revised manuscript received 1 November 1978)

The isobaric analog resonance in ^{57}Co , corresponding to the $J^\pi = 9/2^+$ parent state at 2.454 MeV in ^{57}Fe , has been located and its γ decay to various T_c levels studied by means of the $^{56}\text{Fe}(p,\gamma)^{57}\text{Co}$ reaction. We have identified the level at 4.597 MeV in ^{57}Co as the antianalog state with $J^\pi = 9/2^+$. Additional information on the $M1$ strength systematics in the isovectorial $9/2^+ \rightarrow 9/2^+$ transitions in the f - p shell nuclei is provided.

NUCLEAR REACTIONS $^{56}\text{Fe}(p,\gamma)^{57}\text{Co}$, $E_p = 3.7\text{--}3.8$ MeV; measured E_γ , $\sigma(E_\gamma, \theta)$, $\Gamma_p \Gamma_\gamma / \Gamma_{\text{tot}}$. ^{57}Co deduced $E1$ and $M1$ strengths. $9/2^+$ analog and anti-analog states. Enriched target.

I. INTRODUCTION

The study of the γ decay of isobaric analog resonances (IAR) has yielded important information in regard to the nuclear structure of parent and analog nuclei. For the isovectorial $M1$ transitions, the spin part of the matrix element is closely related to that in Gamow-Teller (GT) β decay. This feature has been very useful in determining the nature of the hindrance factor in the β decay of certain medium-mass nuclei.^{1,2} The hindrance factor in such nuclei can be understood in terms of the particle-hole excitations in the target nucleus. The GT or the isovectorial spin part of the $M1$ operator $\sum \tau_j \sigma_j$, acting on the ground state (g. s.) configuration of the even-even nucleus can generate core polarized states (CPS) of the type $[(\pi f_{7/2})(\nu f_{7/2})^{-1}]_{1^+}$ and spin-flip states (SFS) of the type $[(\pi f_{5/2})(\nu f_{7/2})^{-1}]_{1^+}$. The CPS and SFS in an even-odd nucleus are obtained by coupling the spin j of the extra nucleon to such core states. Transitions to the CPS and SFS may be energetically forbidden in β decay. In such cases they may still be observed in the γ decay of the IAR. In ^{63}Cu , for example, they are shown to account for a significant part of the missing GT (or $M1$) strengths.³

By definition the IAR and the anti-isobaric-analog states (AIAS) have the same particle-hole components as the CPS and SFS but which are coupled to 0^+ in the target nucleus. The CPS and SFS are found to have an important hindrance effect on the $M1$ strength in the IAR \rightarrow AIAS transition. The $p_{3/2}$ IAR transition strength in the f - p shell⁴ is found to be hindered by a factor of 100 or more compared to the single particle (s.p.) value (for the definition

of s.p. estimates see Ref. 6). Exceptions to the hindered $M1$ transitions are the IAR \rightarrow AIAS transitions having parent states of positive parity, e.g., $\frac{5}{2}^+$ and $\frac{9}{2}^+$. The $\frac{9}{2}^+$ state in particular has attracted a great deal of attention and has resulted in a fairly systematic study of the associated $M1$ strength.

For the copper isotopes ($A = 59 \sim 63$) the strength of $g_{9/2}$ IAR \rightarrow AIAS transition (Ref. 5 and references therein) is in the range of 10 \sim 20% of the s.p. estimates, gradually increasing with the mass number. On either side of these nuclei, however, the strength of this transition seems to be reduced. For example, at the upper end of the $1f$ - $2p$ shell^{5,7} this value is reduced to 0.3% in ^{69}Ga and to 0.03% in ^{73}As . At the lower end, in the case of ^{55}Co , the value is 5% of the s.p. estimate.⁸ This observation can be qualitatively understood as an increasing core polarization effect as one departs from the closed $f_{7/2}$ proton shell targets. To better understand this phenomenon and to complete the $M1$ strength systematics, further data on target nuclei whose $1f_{7/2}$ proton shell is not completely filled would be very useful. With this in view, we studied the $^{56}\text{Fe}(p,\gamma)^{57}\text{Co}$ reaction to locate the $\frac{9}{2}^+$ IAR and AIAS and investigated the decay of the IAR.

II. EXPERIMENTAL PROCEDURE AND RESULTS

A. Details of measurements and resonance identification

Isotopically enriched (99%) ^{56}Fe targets of about $20 \mu\text{g}/\text{cm}^2$ thickness, vacuum evaporated on $20 \mu\text{g}/\text{cm}^2$ thick carbon backing, were bom-

barded with the proton beam of the Université Laval Van de Graaff accelerator. A 50 cm³ Ge(Li) detector, with a resolution of about 3 keV for 1.33 MeV γ rays, was used to detect the γ rays from the $^{56}\text{Fe}(p,\gamma)^{57}\text{Co}$ reaction. Details of the target chamber, the detection system, and the experimental procedure have been described earlier.^{3,7} The overall resolution of the system, including the beam spread and excluding target thickness effects, was around 1 keV.

From the proton binding energy in ^{57}Co and the excitation energy of the parent state in ^{57}Fe , the γ -ray energy for the transition from the IAR of the $\frac{9}{2}^+$ state of ^{57}Fe to the $\frac{7}{2}^-$ ground state (g.s.) of ^{57}Co was estimated to be 9.7 MeV; consequently, although the whole spectrum was recorded, a window was set to count γ rays between 8.6 and 9.7 MeV. The excitation function for these γ rays was obtained in 1 keV steps for the proton energy region of 3.70 to 3.76 MeV where the analog of the $\frac{9}{2}^+$ state is anticipated. In this region two resonances were observed at 3.721 and 3.728 MeV, with an intense γ -ray transition to the ground state (Fig. 1). The resonance at 3.721 MeV was found to populate also the $J^\pi = \frac{3}{2}^-$ level at 1.757 MeV and no transition feeding other high spin

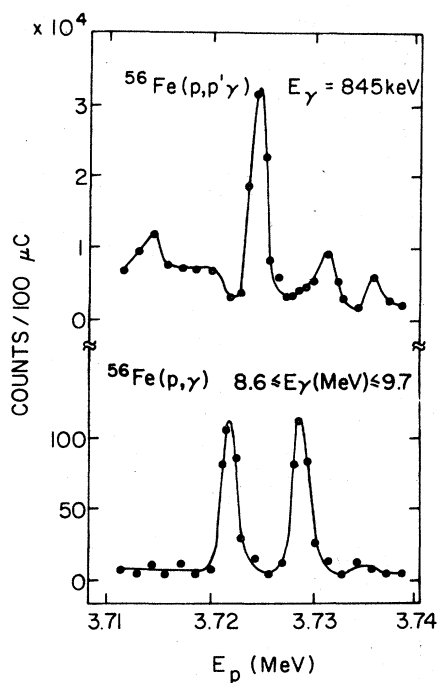


FIG. 1. Excitation functions for $(p, p'\gamma)$ and $R \rightarrow \text{g.s.}$ transition in the $^{56}\text{Fe}(p, \gamma)^{57}\text{Co}$ reaction taken simultaneously with the Ge(Li) detector. Solid lines are drawn only to guide the eye.

states was observed with significant strength. Hence we ruled this out as a candidate for the $\frac{9}{2}^+$ IAR. On the other hand, the resonant level (R) for $E_p = 3.728$ MeV was found to decay only to known high spin states $g_s(\frac{7}{2}^-)$, $1.223(\frac{9}{2}^-)$ and to the state at 4.597 MeV. The on resonance γ -ray spectrum is shown in Fig. 2. A spectrum recorded off resonance showed no primary radiation to these levels; it consisted mainly of fluorine radiation. Hence this resonance is most likely the $\frac{9}{2}^+$ IAR.

The 4.597 MeV state can be identified with the one observed by Rosner and Holbrow⁹ at 4.60 ± 0.02 MeV in the $^{56}\text{Fe}(^3\text{He}, d)^{57}\text{Co}$ reaction. Since this state was populated by an $l = 4$ proton transfer the possible J^π values are limited to $\frac{7}{2}^-$ or $\frac{9}{2}^+$. In the present study this state was observed to decay only to the $\frac{7}{2}^-$ state at 2.311 MeV and the $\frac{7}{2}^-$ gs of ^{57}Co .

The angular distributions of primary γ rays, between 0 and 90 degrees, were obtained for the $R \rightarrow g_s(\frac{7}{2}^-)$, $R \rightarrow 1.223$ MeV ($\frac{9}{2}^-$), and $R \rightarrow 4.597$ MeV ($\frac{7}{2}^+$, $\frac{9}{2}^+$) transitions as well as those of the secondary γ rays for the $4.597 \rightarrow 2.311$ MeV ($\frac{7}{2}^-$) and the $4.597 \rightarrow g_s(\frac{7}{2}^-)$ transitions.

B. Extraction of transition strengths

Since there are two closely lying resonances feeding the ground state, we used the thin target excitation function to extract the strength $\Gamma_p \Gamma_\gamma / \Gamma_{\text{tot}}$. As to be seen from Fig. 1, the peak to valley ratio is about 50:1 and thus any background interference in the resonance is considered negligibly small. Also, absence of g.s. and other transitions in the long spectrum accumulated off resonance supports this conclusion. To extract the g.s. transition strength, the yield for the full energy and two escape peaks, with proper background subtraction, was used. This yield is closely 0.37 times the

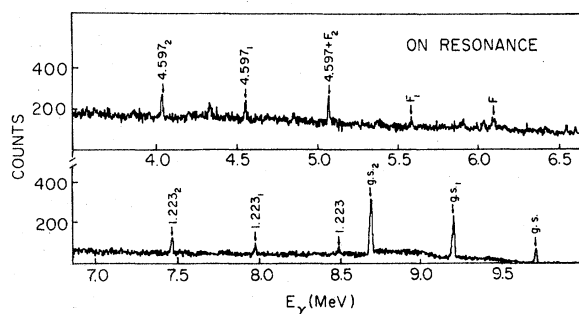


FIG. 2. On resonance γ -ray spectrum at $E_p = 3.728$ MeV. F is the γ ray from traces of fluorine contamination.

TABLE I. γ -decay properties of the $\frac{9}{2}^+$ IAR in the $^{56}\text{Fe}(p, \gamma)^{57}\text{Co}$ reaction.

Transition	$\Gamma_p \Gamma_\gamma / \Gamma_{\text{tot}}$ (eV)	$B(E1)^a$ ($e^2 f^4$)	$B(M1)^a$ (μ_n^2)	$\frac{\Gamma_\gamma(\text{exp})^a}{\Gamma_\gamma(\text{s.p.})}$
IAR \rightarrow g.s. $\frac{9}{2}^+ \rightarrow \frac{7}{2}^-$	0.137 ± 0.020	1.44×10^{-4}		
IAR $\rightarrow 1.223$ $\frac{9}{2}^+ \rightarrow \frac{9}{2}^-$	0.029 ± 0.005	4.56×10^{-5}		
IAR $\rightarrow 4.597$ $\frac{9}{2}^+ \rightarrow \frac{9}{2}^+$	0.029 ± 0.006		1.89×10^{-2}	0.011

^a Assuming $\Gamma_{\text{tot}} \approx \Gamma_p \gg \Gamma_\gamma$.

one seen in Fig. 1. This factor is found to be consistent with the value extracted directly from the long spectrum shown in Fig. 2. From the g.s. strength thus extracted and from the measured branchings, partial strengths were also deduced for the $R \rightarrow 1.223$ MeV and $R \rightarrow 4.597$ MeV transitions (Table I).

It is to be noted that the resonant state is bound with respect to neutron emission and that α emission is severely hindered by the Coulomb barrier. The total resonance width (Γ_{tot}) thus results mainly from the elastic, the inelastic, and the (p, γ) channels. As the proton elastic and inelastic widths are not known, it is not possible to evaluate $\Gamma_p / \Gamma_{\text{tot}}$. The assumption $\Gamma_{\text{tot}} \approx \Gamma_p$ provides a lower limit for Γ_γ , whereas the possibility $\Gamma_p \approx \Gamma_\gamma$ gives the upper limit for Γ_γ , which is at most two times the lower limit. Table I gives the $B(E1)$ and $B(M1)$ values deduced with the conventional $\Gamma_{\text{tot}} \approx \Gamma_p$ assumption.

III. DISCUSSION

A. Spin determination of the 9.690 MeV resonance (R)

The experimental angular distributions were fitted to the theoretical functions calculated using the formalism of Rose and Brink.¹⁰ Different spins J_R for the resonance and $\frac{7}{2}$ and $\frac{9}{2}$ spin possibilities for the 4.597 MeV level were assumed. The fact that R decays selectively to high spin states restricts its spin to values between $\frac{5}{2}$ and $\frac{11}{2}$. The analysis of the $R \rightarrow$ g.s. ($\frac{7}{2}^-$) transition gave no solution with a χ^2 value below the 0.1% confidence limit for the spin values of $\frac{7}{2}$ and $\frac{11}{2}$. The results are shown in Fig. 3 for the remaining $\frac{5}{2}$ (dashed lines) and $\frac{9}{2}$ possibilities (solid lines). The $\frac{5}{2}$ possibility is quite unlikely for the following reasons: If R is assumed to be of positive parity it implies an $M2$ strength of greater than 3 W.u. for the $R \rightarrow 1.223$ MeV ($\frac{9}{2}^-$) transition. If

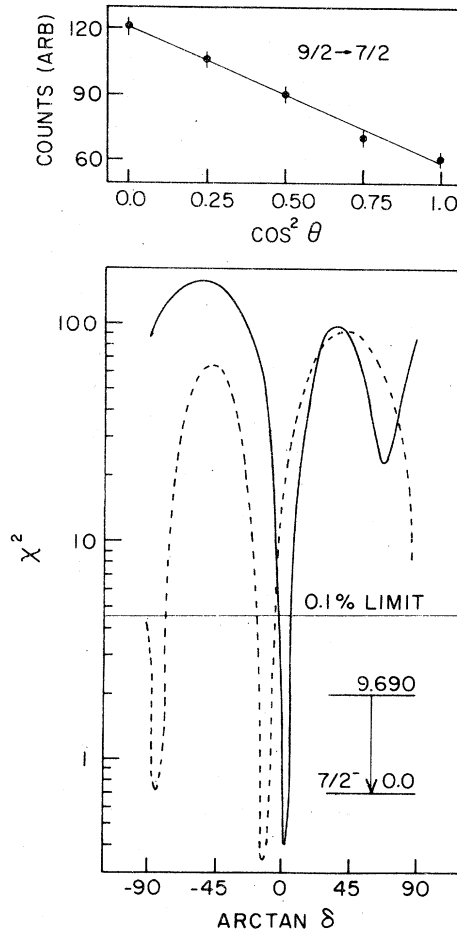


FIG. 3. (top) Fit to the $R \rightarrow$ g.s. ($\frac{7}{2}^-$) angular distribution and (bottom) the χ^2 plot versus the mixing ratio for an assumed spin of $\frac{5}{2}$ (dashed line) and of $\frac{9}{2}$ (solid line).

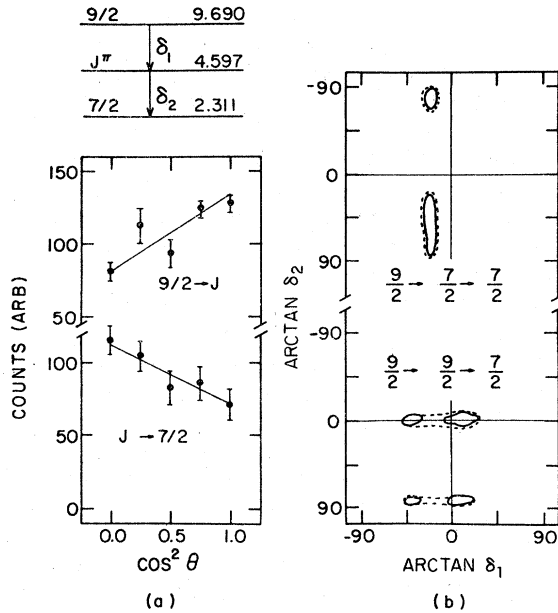


FIG. 4. (a) Angular distribution fits to the primary ($R \rightarrow 4.597$ MeV) and the secondary (4.597 MeV $\rightarrow 2.311$ MeV) transitions. (b) The χ^2 contour lines as a function of $\arctan \delta_1$ and $\arctan \delta_2$ for the $\frac{7}{2}^-$ (top) and the $\frac{9}{2}^+$ (bottom) possibilities for the 4.597 MeV state. The mixing ratios for the primary and the secondary transitions are denoted by δ_1 and δ_2 . The solid and dashed lines correspond to 0.1% and 1% probability limits.

negative parity is assumed, it would result in an $M2$ strength of about 40 W.u. for the $R \rightarrow 4.597$ MeV ($\frac{9}{2}^+$) transition. These large $M2$ strengths are very improbable. The Coulomb displacement energy, $\Delta E_c = 8.877 \pm 0.005$ MeV, calculated at the resonance energy, is in good agreement with recent compilations by Courtney and Fox¹¹ and thus provides additional support that R is the $\frac{9}{2}^+$ IAR. In the following, $J_R^{\pi} = \frac{9}{2}^+$ is adopted. The $R \rightarrow$ g.s. transition is mostly pure $E1$ in nature ($\delta = 0.05_{-0.07}^{+0.1}$).

B. Spin determination of the 4.597 MeV state

The primary and secondary γ -ray angular distributions in the $R(\frac{9}{2}^+) \rightarrow 4.597$ MeV ($\frac{7}{2}^-$ or $\frac{9}{2}^+$) $\rightarrow 2.311$ MeV ($\frac{7}{2}^-$) cascade are discussed here. In Fig. 4(a), the curves represent the fits obtained with the best mixing ratios δ_1 and δ_2 to the experimental angular distributions. The χ^2 contour lines in the $\arctan \delta_1$ - $\arctan \delta_2$ plane are shown in Fig. 4(b) for the possible $\frac{7}{2}^-$ and $\frac{9}{2}^+$ spins of the 4.597 MeV state. The dashed and solid lines correspond to the 0.1% and 1% probability limit. The spin sequence $\frac{9}{2}^+ \rightarrow \frac{7}{2}^- \rightarrow \frac{7}{2}^-$ yields very large mixing ratios ($\delta_1 = -0.36 \pm 0.09$, $\delta_2 = 0.84_{-0.26}^{+0.6}$) im-

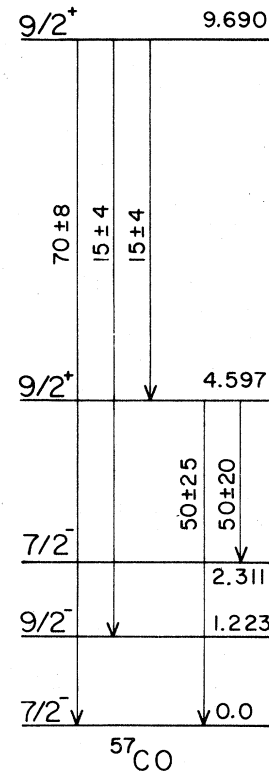


FIG. 5. γ decay scheme of $\frac{9}{2}^+$ IAR in ^{57}Co (only relevant levels in ^{57}Co are shown).

plying considerable $E2$ and $M2$ mixings in the primary and secondary transition, respectively. Hence the $J = \frac{7}{2}^-$ assignment is rejected. Assuming $\frac{9}{2}^+$, the solutions obtained are consistent with a pure $M1$ primary transition ($\frac{9}{2}^+ \rightarrow \frac{9}{2}^+$, $\delta_1 = 0.18_{-0.37}^{+0.18}$), followed by a pure $E1$ transition ($\frac{9}{2}^+ \rightarrow \frac{7}{2}^-$, $\delta_2 = 0.18 \pm 0.18$). We can therefore identify the $R(\frac{9}{2}^+) \rightarrow 4.597$ MeV ($\frac{9}{2}^+$) as an analog-antianalog transition (Fig. 5). From the observed splitting of these two states we obtain a value of 112 MeV for the symmetry potential consistent with the value given by Lane¹² for nuclei in this mass region.

C. $M1$ strength in the $9/2^+$ IAR \rightarrow AIAS transition

The Table I shows the reduced width $B(M1)$ and the corresponding $\Gamma_{\gamma}(\text{exp})/\Gamma_{\text{s.p.}}$ value for the IAR \rightarrow AIAS transition as well as the $B(E1)$ values for other transitions. The experimental to the s.p. width ratio of 0.01 that we obtain for ^{57}Co is smaller than the value of 0.05 obtained for ^{55}Co by Martin *et al.*⁸ The general reduction of $M1$ strength in the copper isotopes¹³ as well as in ^{55}Co has been attributed to the mixing of CPS into the AIAS. A similar effect could be present in

the ^{57}Co case. However, the further reduction in ^{57}Co , as compared to that in ^{55}Co , is unlikely to arise from an increased fragmentation of the AIAS since the spectroscopic factors $S(^3\text{He}, d)$ for the AIAS is about 0.5 in both cases^{14, 15}; it is worth noting that the $\frac{9}{2}^+$ IAR populates only a single positive parity state ($\frac{9}{2}^+$) in ^{57}Co . The reduction we observe could be attributed to the fragmentation of the parent state in ^{57}Fe as discussed below. In the case of ^{57}Co , the target nucleus ^{56}Fe with two valence neutrons in the $1f_{5/2}$, $2p_{3/2}$, and $2p_{1/2}$ shells is known to exhibit a more collective nature than ^{54}Fe with no valence neutrons. For example,¹⁶ the first 2^+ state in ^{56}Fe occurs at 0.847 MeV with quadrupole deformation parameter (β_2) of 0.23, whereas in ^{54}Fe the corresponding level is at 1.413 MeV with $\beta_2 = 0.18$. This is also reflected in the spectroscopic factors $S(d, p)$: the value for the $\frac{9}{2}^+$ parent state in ^{55}Fe is 0.7, while it is only 0.4 for the corresponding level in ^{57}Fe (Refs. 14 and 15).

In conclusion, we note that the $M1$ strength in

the $g_{9/2}$ analog-antianalog transitions reaches a maximum in the middle of the f - p shell and tends to fall off on either side. Qualitatively, we can interpret this feature as due to increasing core-polarization effects as one departs from the closed $f_{7/2}$ proton shell targets. There are, however, considerable deviations from one nucleus to another and to understand these in a more quantitative manner, shell model calculations with particles occupying the $1f_{7/2}$, $2p_{3/2}$, $1f_{5/2}$, $2p_{1/2}$, and $1g_{9/2}$ orbits are necessary. Only such calculations can throw light on the important question of the isovectorial $M1$ strength distribution in this region.

The authors would like to thank Dr. S. Ramavataram for many valuable suggestions and critical reading of the manuscript. The efficient operation of the accelerator by the Van de Graaff crew is very much appreciated. This work was supported by the National Research Council of Canada.

*Deceased on Dec. 29, 1977.

¹C. Gaarde, K. Kemp, Y. V. Naumov, and P. R. Amundsen, Nucl. Phys. **A143**, 497 (1970).

²C. Gaarde, K. Kemp, C. Petresch, and F. Folkmann, Nucl. Phys. **A184**, 241 (1972).

³K. Ramavataram, C. S. Yang, G. F. Mercier, C. St-Pierre, and D. Sykes, Phys. Rev. C **9**, 237 (1974).

⁴H. V. Klapdor, Phys. Lett. **35B**, 405 (1971).

⁵M. Schrader, H. V. Klapdor, G. Bergdolt, and A. M. Bergdolt, Phys. Lett. **60B**, 39 (1975).

⁶S. Maripuu, Nucl. Phys. **A123**, 357 (1969).

⁷K. Ramavataram, C. Rangacharyulu, I. M. Szöghy, R. Hilko, and C. St-Pierre, Phys. Rev. C **17**, 1583 (1978).

⁸D. J. Martin, W. McLatchie, B. C. Robertson, and J. Szücs, Nucl. Phys. **A258**, 131 (1976).

⁹B. Rosner and C. H. Holbrow, Phys. Rev. **154**, 1080 (1967).

¹⁰H. J. Rose and D. M. Brink, Rev. Mod. Phys. **39**, 306 (1967).

¹¹W. J. Courtney and J. D. Fox, At. Nucl. Data Tables **15**, 141 (1975).

¹²A. M. Lane, Phys. Rev. Lett. **8**, 171 (1962).

¹³G. Bergdolt, A. M. Bergdolt, H. V. Klapdor, and M. Schrader, Nucl. Phys. **A263**, 477 (1976).

¹⁴D. C. Kocher, Nucl. Data Sheets **18**, 463 (1976).

¹⁵R. L. Auble, Nucl. Data Sheets **20**, 253 (1977).

¹⁶P. H. Stelson and L. Grodzins, Nucl. Data **1**, 21 (1965).